Thermochimica Acta, 47 (1981) 27—36
Elsevier Scientific Publishing Company, Amsterdam — Printed in Belgium

STRUCTURAL CHANGES AND SURFACE PROPERTIES OF THERMALLY TREATED CERIC OXIDE HYDRATE

SUZY A SELIM and MOHAMED I. ISMAIL

Chemistry Department, Faculty of Science, Ain Shams University, Cairo (Egypt)

(Received 7 January 1981)

ABSTRACT

Surface area measurements were carried out by N_2 adsorption at 77 K on two batches of hydrous ceric oxide prepared under a continuous change of pH, 10.78 → 9 50, (C_1) and at a constant pH of 10.78 (C_2). Dehydration products were obtained at various temperatures up to 800°C. Structural and phase changes were studied by X-ray diffraction (XRD), differential thermal analysis (DTA) and thermogravimetry analysis (TGA).

DTA and TGA of both samples showed the existence of a large endotherm at 150°C responsible for the evolution of one water molecule associated with the oxide. Two small exotherms also appear in the temperature range 300—350°C, followed by a small endotherm at 455°C; explanations for their presence are given

Products obtained at temperatures ≤210°C were amorphous to X-rays. In the temperature range 310—400°C some intermediate oxides between CeO_2 and Ce_2O_3 develop with a poorly crystalline structure and possessing *d*-distances in the ranges 3.080—3.020 Å, 1.957—1.926 Å and 1.903—1 888 Å. Stabilization of the CeO_2 structure occurs at temperatures ≥490°C. Samples from batch C_2 always possessed higher areas than the corresponding samples from batch C_1.

Pore structure analysis showed the original parent material of both samples to be microporous. Mesoporosity gradually develops at temperatures ≥400°C and ≥110°C for samples C_1 and C_2, respectively Sample C_2 gives rise to products with a stable average pore size of ~13.53 Å in the temperature range 400—800°C.

INTRODUCTION

Cerium, technically the most important member of the cerite group, exhibits a great similarity in its aqueous phase and tetravalent state to that of Zr(IV) [1], which forms its oxide hydrate by a polymerization process in solution. For such systems [2] the coordination of oxygen changes upon dehydration of the gel, resulting in a considerable rearrangement of the atoms in the particles which could produce materials active with respect to sintering [3]. This gives hydrous ceric oxide a potential use as a good adsorbent or catalyst in which the surface structure is of vital importance.

Ceric oxide, mixed with other oxides, is used as a catalyst for the synthesis of methanol [4], in several oxidation processes [5,6], and is also used as a decolorizer of flint glass [7].

Surface studies of pure CeO_2 were completely neglected until 1978 when Rao [8] carried out some adsorption and electrical conductivity studies in oxygen atmospheres. The adsorption was defined by the Freundlich adsorp-

tion isotherm and from the conductivity measurements he concluded that CeO_2 is an *n*-type semiconductor. No other textural studies were reported and such details needed to be explored.

The precipitation of the oxides is an important step in its preparation, since surface area, pore size and resistance against sintering are parameters strongly dependent upon precipitation conditions. The aim of the present investigation is to reveal the relation between the surface texture and the effect of change of pH during precipitation on the solid material using such techniques as N_2 adsorption, X-ray diffraction (XRD), differential thermal analysis (DTA) and thermogravimetric analysis (TGA).

EXPERIMENTAL

Materials

Two batches of Ce(IV) oxide hydrate were prepared. A 1 M solution of ammonium ceric nitrate (A.R.) was flushed from a douche to a slight excess of a well-stirred 4 M NH_4OH solution at room temperature (<30°C). The initial pH was 11.5 which dropped to 9.5 after complete precipitation. The precipitate was further stirred for 30 min, then filtered and thoroughly washed till free from NO_3^- and dried to constant weight at room temperature in the presence of an air current. This batch will be designated C_1.

A second batch, C_2, was prepared by the same method, but the pH was kept constant at 10.78 throughout the precipitation process by NH_4OH solution. An initial drop from 11.5 (pH of NH_4OH solution) to 10.78 took place. The precipitate was further treated as C_1.

Both samples, C_1 and C_2, proved, by chemical analysis, to be free from any ammonium ions or adsorbed ammonia. Dehydration products were obtained for the above samples by heating in the temperature range ambient—800°C for 2 h in the presence of air. The treatment temperature will always follow the preparation symbol between parentheses.

Apparatus and technique

TG analysis was carried out in the presence of both static air and nitrogen atmosphere flowing at a rate of 5 cc min^{-1} using a Stanton-Redcroft thermobalance type 750/770 connected to a BD 9 two-channel automatic recorder "Kipp and Zonnen" at a heating rate of 10°C min^{-1}.

DTA was carried out using high-temperature α-alumina as inert standard, and a program temperature controller "Ether" transitrol type 994/2 was used to permit a linear rate of heating being 10°C min^{-1} together with a Cambridge Recorder Model "B" for recording the temperature difference.

The X-ray diffraction patterns were obtained using a Philips diffraction unit, Model PW 1010 using Ni-filtered Cu radiation. The *d*-distances were calculated and compared with their relative intensities with data in the ASTM cards [9,10].

Adsorption—desorption isotherms of nitrogen at 77 K were determined

by conventional volumetric gas adsorption. Surface areas calculated by the BET method, and signified as S_{BET}, used the value of 16.2 Å^2 as the molecular area of adsorbed nitrogen.

RESULTS AND DISCUSSION

Structural characterization

TG analysis of preparations C_1 and C_2 under both air and nitrogen atmospheres showed a continuous loss in weight commencing at ~50°C and terminating at ~650°C. Three main regions are distinguished, one at about 100°C, another covering a temperature range of ~100—~320°C, followed by a terminating step up to 650°C [Fig. 1 curve (a)]. The absence of any stepwise loss was confirmed upon reducing the heating rate to 1°C min^{-1} in both atmospheres. The total loss in weight was identical for both samples (~16.6%). The percentage losses for the thermally dehydrated samples from C_1 and C_2 are given in Tables 1 and 2, respectively.

The DTA curves produced for both samples were similar and showed a large endothermic peak centered at ~150°C, with a distinct shoulder at ~100°C [Fig. 1 curve (b)]. This shoulder coincides with the first region of water evolution observed in the TG curves and corresponds to the evolution of the adsorbed water from the surface of the samples. The endotherm at ~150°C results from the evolution of the water bound to the solid material and corresponds to the second region of water loss in the TG curves, which extends to higher temperatures covering the third region for that water situated in the bulk. About one water molecule is believed to be attached to CeO_2, namely $CeO_2 \cdot H_2O$ [or $CeO(OH)_2$], besides the adsorbed water. XRD patterns showed the parent gel and those heated at 110°C and 210°C to be

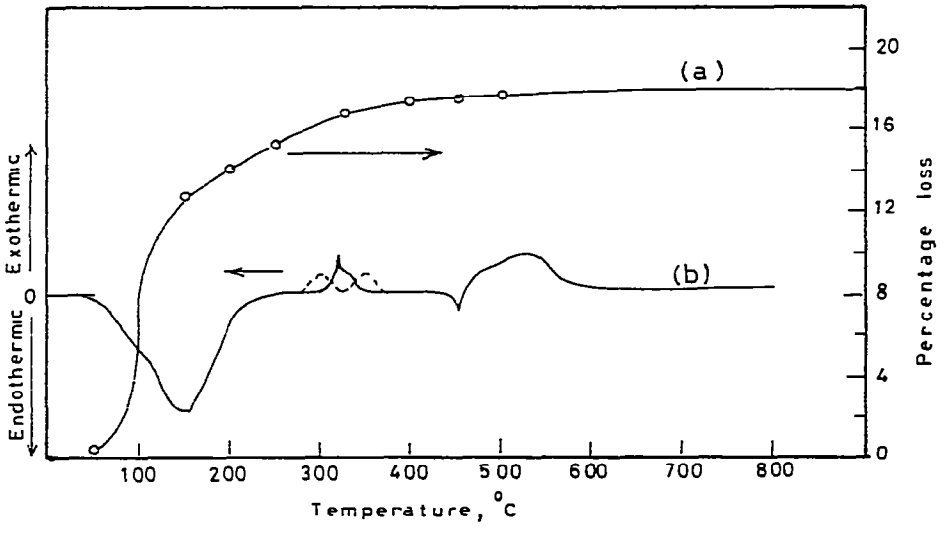

Fig 1 Thermogravimetric curve (a) and differential thermal curve (b) for hydrous ceric oxide, sample C_1.

TABLE 1

Surface characteristics of hydrous ceric oxide, sample C_1, and its thermally dehydrated products

Sample	% Water loss	BET-c constant	S_{BET} ($m^2\ g^{-1}$)	S_t ($m^2\ g^{-1}$)	$V_{p_{0.95}}$ ($ml\ g^{-1}$)
C_1 (original)		53	164.5	158.5	0.1911
C_1 (110)	9.87	62	175.1	168.0	0.1880
C_1 (210)	14.05	69	156.2	157.0	0.1833
C_1 (310)	15.88	39	131.7	130.5	0.1499
C_1 (400)	16.29	15	145.3	145.0	0.1958
C_1 (600)	16.59	18	97.9	102.0	0.1150
C_1 (800)	16.59	6	87.5	85.0	0.1127

partially amorphous showing no distinct peaks but very broad bands corresponding to the peaks produced by samples heated at higher temperatures (Fig. 2), i.e. they possessed a poorly developed framework from which the crystal unit is formed at higher temperatures.

After completion of the endothermic effect, two small consecutive exothermic peaks are observed in the DTA curves at ~300°C and 350°C [dotted in Fig. 1 curve (b)] which are replaced by a sharp exothermic effect at ~320°C, with a small shoulder at 335°C upon aging for about 6 months. These exotherms, though small, are reproduced in each repeated DTA run. From XRD data for samples heated at 310°C and 400°C (2 h each) from samples C_1 and C_2, a series of peaks forming bands in the d-distance ranges of 3.080—3.020 Å, 1.957—1.926 Å, and 1.903—1.888 Å are observed, besides those characteristic for CeO_2, varying slightly in intensities for the two preparations (Figs. 2 and 3). These values of d-distances are close to those for the trivalent oxide [9,10], which indicate the existence of some intermediate oxides between CeO_2 and Ce_2O_3 similar to Pr(IV) [11,12], a

TABLE 2

Surface characteristics of hydrous ceric oxide, sample C_2, and its thermally treated products

Sample	% Water loss	BET-c constant	S_{BET} ($m^2\ g^{-1}$)	S_t ($m^2\ g^{-1}$)	$V_{p_{0.95}}$ ($ml\ g^{-1}$)
C_2 (original)		68	214.7	214.0	0.2346
C_2 (110)	10.60	61	204.2	194.0	0.2346
C_2 (210)	14.16	26	207.1	212.0	0.2556
C_2 (310)	15.01	25	160.8	164 5	0.1920
C_2 (400)	15.74	14	152.9	148.0	0.1998
C_2 (600)	16.58	8.5	114.5	112.0	0.1523
C_2 (800)	16.58	6.4	89.7	85.0	0.1197

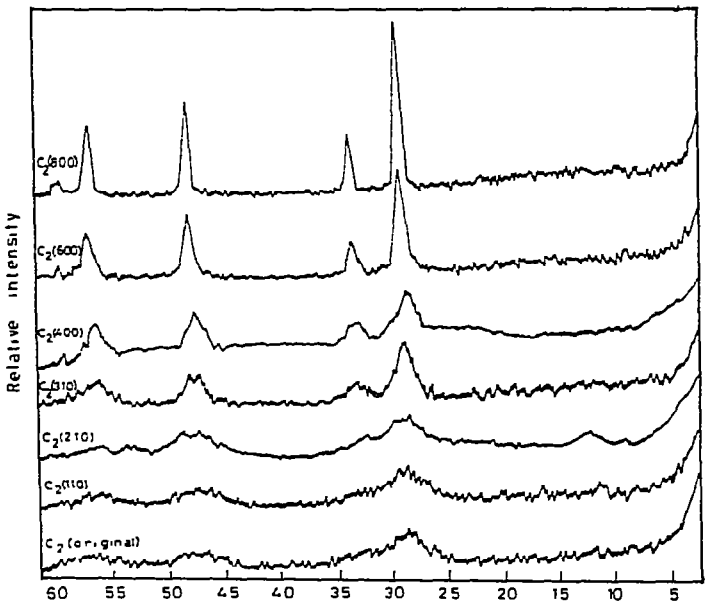

Fig 2 X-Ray diffraction patterns for ceric oxide hydrate, sample C_2, and its thermal decomposition products

member of the cerite group. Accordingly, these exotherms seem to result from two consecutive auto-reduction processes, viz.

$$4\ Ce^{4+} + e \rightarrow 4\ Ce^{3.75+}\ (Ce_8O_{15})$$

and

$$4\ Ce^{3.75+} + e \rightarrow 4\ Ce^{3\ 5+}\ (Ce_4O_7)$$

Such auto-reduction processes were previously noted for other oxide systems [13 -15].

At 455°C, a small but sharp endothermic effect is produced which results from the oxidation of the reduced oxide to CeO_2.

At ~525°C, a large broad exotherm is present with a shoulder at ~490°C.

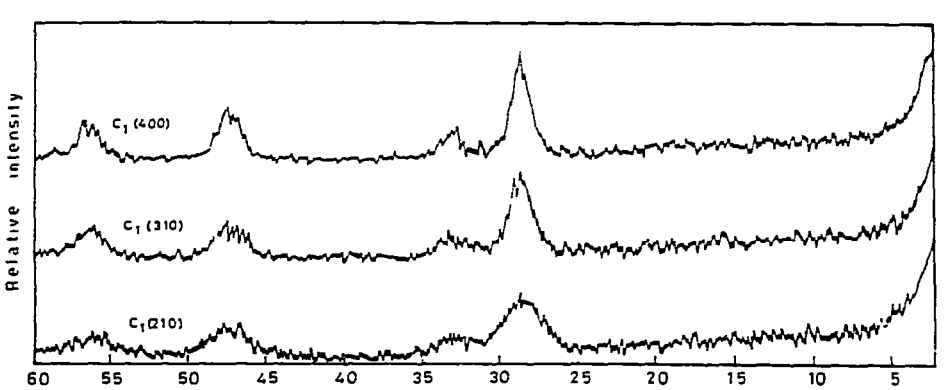

Fig. 3. X-Ray diffraction patterns for ceric oxide hydrate, sample C_1, heated in the temperature range 210—400°C.

XRD patterns of samples C_1 and C_2 heated at 600° C and 800° C show them to be well crystallized cubic CeO_2 (Fig. 2). The shoulder at ~490° C seems to be associated with the establishment of the crystalline structure of CeO_2 formed from the pseudolattice of the original material. Following crystallization to the stable form, a marked decrease in area is usually observed [16, 17] and was actually found in the present investigation. This is manifested in the broad exotherm of the DTA curves at about 525° C resulting from the decrease in surface energy.

Surface area and pore structure

Adsorption—desorption isotherms of N_2 at —196° C were obtained for the two preparations of hydrous ceric oxide, C_1 and C_2, as well as their thermally treated products. The adsorption isotherms of all the samples were type II and exhibit closed hysteresis loops, the closure pressure varying between 0.35—0.50 P/P_0. A typical set of isotherms is shown in Fig. 4 obtained for the adsorption of N_2 gas on sample C_2 and its thermally treated products.

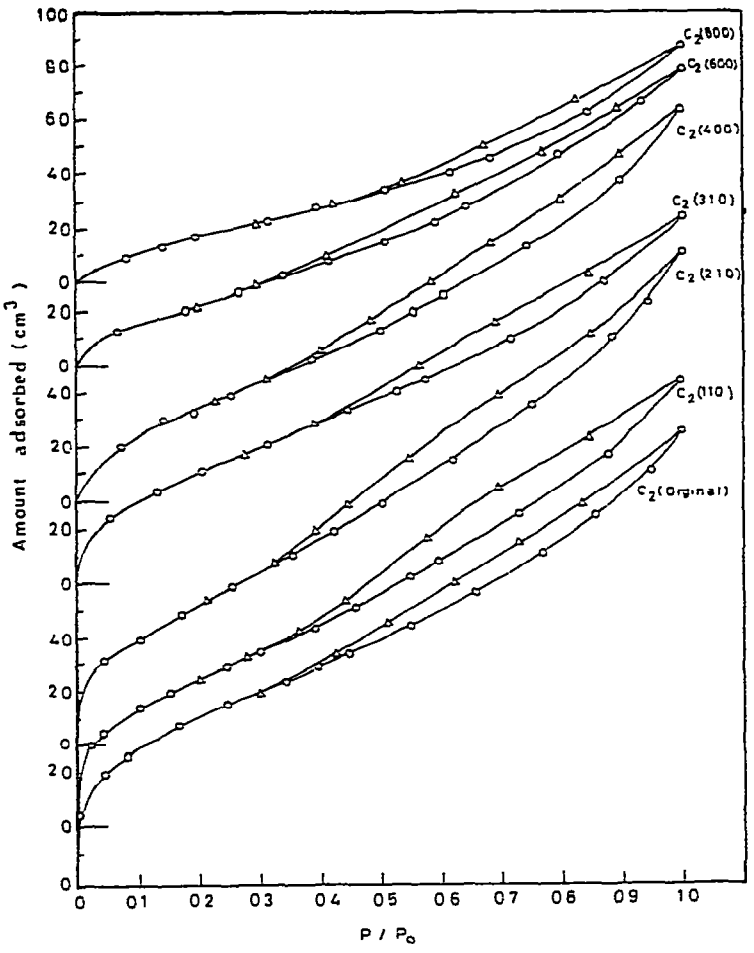

Fig 4. Adsorption—desorption isotherms of nitrogen at —196°C on hydrous ceric oxide, sample C_2, and its thermally treated products.

The specific surface areas were estimated by the application of the BET equation in its normal range of applicability, and are summarized as S_{BET} in Tables 1 and 2 together with their BET-*C* constants. The specific area of sample C_1 increases slightly at 110°C, then decreases by heat treatment to 300°C. A small increase is observed at 400°C, above which the area decreases again. The trend is different for sample C_2 where an initial decrease is observed at 110°C which remains invariably the same at 210°C. Above this temperature, the area decreases continuously up to 800°C but the decrease at 400°C is small (Fig. 5). From TG analysis (Fig. 1), more than 90% of the water is evolved in the temperature range 110—310°C and the surface properties of these low-temperature samples should be dependent on the amount of water retained. As both samples, C_1 and C_2, contain the same amount of water (~16.6%), comparable areas were expected for these samples. However, the areas produced for samples from C_2 are higher than those from preparation C_1, and the amount of water present does not seem to be the sole factor controlling the areas. The only plausible factor would be the particle size — precipitation at constant high pH, as in C_2, produces particles of smaller size than if the pH decreases during the precipitation process, as in C_1, probably resulting from differences in the rate of nucleation of the precipitate.

No significant structural changes are observed for the solid material below

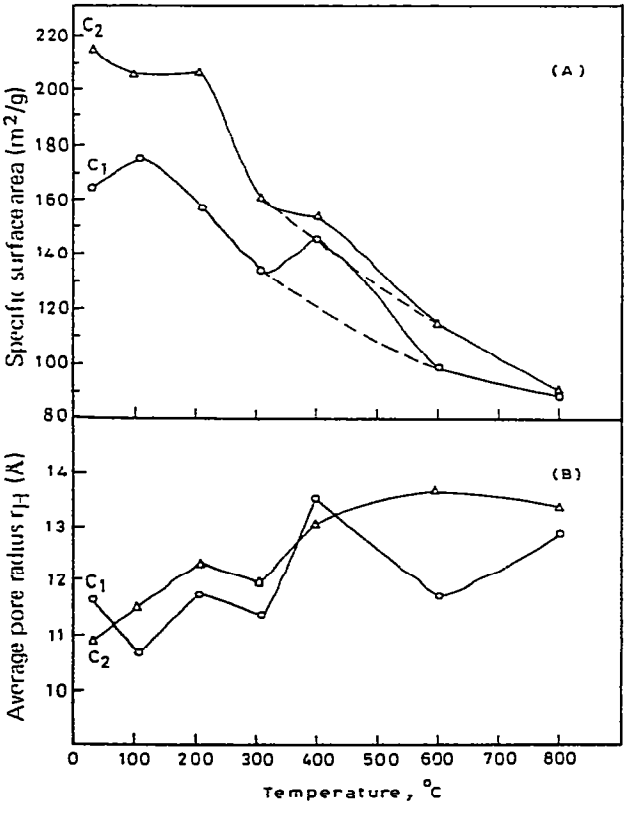

Fig. 5 Variation of (A) specific surface area, S_{BET}, and (B) average pore radius, $\bar{r}_H$, with treatment temperature for samples C_1 (○) and C_2 (△).

300°C (see structural characterization) and the changes in the N_2 areas with dehydration temperature in this range would therefore only result from the variation in pore size as a consequence of the water evolution upon thermal treatment.

The size of the pores, whether meso, micro or a mixture of both, could be demonstrated through the application of the *t*-method of De Boer and co-workers [18]. In these plots, the *t*-curves of Mikhail et al. [19] (BET-*C* constants <30) and De Boer and co-workers [18] (BET-*C* constant ~60) based on non-porous solids with BET-*C* constants matching those of the samples under test were used. The agreement between S_{BET} and S_t (surface area obtained from the V_1—t plot) is observed for all samples (Tables 1 and 2), thus fulfilling the main criterion for the correct choice of *t*-curve used in the analysis. The V_1—t plots constructed for samples C_1 and C_2 and their heated products are shown in Fig. 6(A) and (B). From Fig. 6, it is clear that both original samples from C_1 and C_2 are predominantly microporous showing a downward deviation at *t*-values of ~9 and ~8, respectively. Upon thermal treatment of C_1 at 110°C and 210°C, the downward deviation commences at $t \approx 7$ Å and ≈9 Å, respectively, pointing to the narrowing and subsequent widening of the pores. This situation is different for C_2 (110) and C_2 (210) where mesoporosity is also observed. Upward deviations commencing at $t \approx 5$ and ≈6 are observed for C_2 (110) and C_2 (210) which do not continue but revert back at a *t*-value of 9.5 Å and 10 Å, respectively.

These changes are also reflected in the total pore volume taken at $P/P_0 = 0.95$ ($V_{p_{0\ 95}}$) and average pore radii obtained as $\bar{r}_H = V_{p_{0.95}}/S_{BET}$. For sample C_2, a continuous widening of the pores takes place with thermal treatment where a process of agglomeration is taking place, whereas for C_1, activation is important at 110°C, where more narrow pores are formed, followed by agglomeration at 210°C. At 310°C, the decrease in area observed for both preparations is accompanied by a decrease in both $V_{p_{0.95}}$ (Tables 1 and 2) and $\bar{r}_H$ (Fig. 5), indicating the commencement of a process of "shrinkage".

Similar to other hydrous oxide systems [2], a continuous decrease in area is expected to occur at 400°C (Fig. 5A, dotted lines) if no other factors come to practice. Actually, in the temprature range 310—400°C small structural changes are observed in the DTA curves and XRD patterns (see structural characterization) which are responsible for the area changes produced. These structural changes are accompanied by widening of the pores, as clearly indicated in their V_1—t plots (Fig. 6) and $\bar{r}_H$ data (Fig. 5). The microporous nature of C_1 (310) is mostly destroyed by heating at 400°C, and a small upward deviation at $t \approx 4$ followed by a further increase in slope at $t \approx 6$ is observed, which revert back at $t \approx 12$. This plot points to the coexistence of two different groups of pores. Sample C_2 (400) shows increased mesoporosity over C_2 (310), with two different sized coexisting groups of pores.

At 600°C, $\bar{r}_H$ decreases for sample C_2 but increases for C_1 and the picture is reproduced from their corresponding V_1—t plots. At this temperature, the crystallization to CeO_2 is well established (Fig. 2) and a decrease in area and total pore volume is observed for both samples C_1 and C_2 (Tables 1 and 2) which is also accompanied by a decrease in $\bar{r}_H$ for sample C_1. For sample C_2, the pores present seem to include internally some ink-bottled pores which

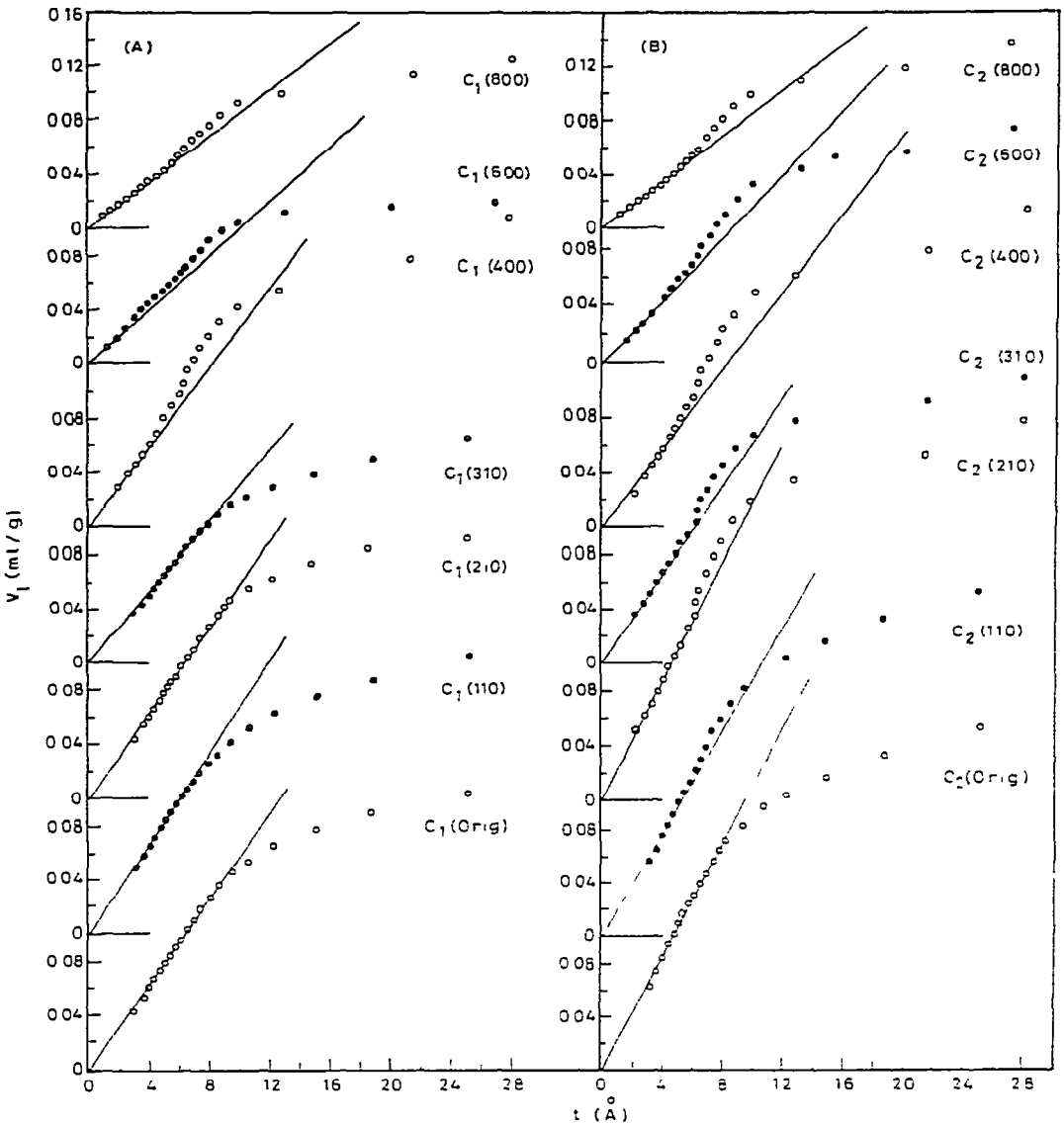

Fig 6 V_1—t plots of samples C_1 and C_2 and their thermally treated products

upon the diminution of their entrances a large internal area is excluded, leaving the outer pore system almost unaffected up to even 800°C. Widening of the pores of sample C_1 at 800°C is apparent where sintering becomes appreciable. Thus, for preparation C_2, an almost stable averaged pore system of ~13.53 Å is obtained in the temperature range 400—800°C, in spite of changes in S_{BET} or V_p.

REFERENCES

1 F.A. Cotton and G. Wilkinson (Eds.), Advanced Inorganic Chemistry, Interscience, New York, 1972

2 S.A. Selim and T M. El-Akkad, J. Appl. Chem. Biotechnol , 27 (1977) 58.
3 B.G. Linsen (Ed.), Physical and Chemical Aspects of Adsorbents and Catalysts, Academic Press, London, New York, 1970.
4 J.C. Ghosh, M.V.C. Sastri and G.S. Kamath, J. Chem. Phys., 49 (1952) 500.
5 S Hillers, E. Poulous, V.A. Slavinskaya, A. Strauthins and M V. Shimanskaya, U S S R. Pat 230,096 (1977); Appl 1,159,180, (1967), Otkrytiya, Izobret. Prom. Obraztsy, Tovarnye Znaki, 54 (27) (1977) 196.
6 F. Huba and I. Malkin, Diamond Shamrock Corp. U.S. Pat 3,819,535 (1974), Appl. 243 823 13 (1972).
7 T.C. Shutt and G Barlow, Am. Ceram Soc Bull , 51 (2) (1972) 155.
8 V. Sitakara Rao, Proc. Indian Natl. Sci. Acad., 43(4) (1978) 254.
9 J.V Smith (Ed), X-Ray Powder Data File and Index to X-ray Data File, Am Soc. Testing Mater , Philadelphia, 1961.
10 Powder Diffraction File, ASTM Alphabetical Index of Inorganic Compounds, International Center for Diffraction Data, Pennsylvania, 1978
11 J M Warmkessel, S H. Lin and L Eyring, Inorg. Chem , 8 (1969) 875
12 S. Renders, K.C. Patel and C.N R Rao, J. Chem Soc A, (1970) 64.
13 S A Selim, Ch A Philip and R Sh. Mikhail, Thermochim. Acta, 36 (1980) 287
14 M. Taniguchi and T R Ingraham, Can. J. Chem., 42 (11) (1964) 2467.
15 J. Bernard and C.R. Theobald, Acad. Sci., 256 (1963) 4916.
16 R Sh Mikhail, S A. Selim and F.I. Zeidan, J. Appl. Chem Biotechnol , 26 (1976) 191
17 T L Webb, in R C. Mackenzie (Ed), Differential Thermal Analysis, Vol. 1, Academic Press, London, New York, 1970
18 B C Lippens, B.G. Linsen and J.H. De Boer, J. Catal., 3 (1964) 32. J.H. De Boer, B G Linsen and Th J Osinga, J. Catal., 4 (1965) 643. B.C. Lippens and J.H. De Boer, J. Catal., 4 (1965) 319.
19 R.Sh. Mikhail, N M Guindy and S. Hanafi, Egypt J. Chem , Special Issue "Tourky", (1973) 53